

## ***Electronic Supplementary Information***

### **Nanonstructural Investigation of Orthogonally-Stacked Mesoporous Silica Films and the Reactivity with Phosphate Buffer**

Reo Kimura <sup>a</sup>, Yadong Chai <sup>b</sup>, Rin Nakajima <sup>a</sup>, Kenichiro Kosugi <sup>c</sup>, Motohiro Tagaya <sup>a</sup>,

\*

<sup>a</sup> *Department of Materials Science and Bioengineering Technology, Nagaoka University of  
Technology, Kamitomioka 1603-1, Nagaoka 940-2188, Japan*

<sup>b</sup> *Department of Materials Science and Engineering, Tokyo Institute of Technology, 4259  
Nagatsuta-cho, Midori-ku, Yokohama 226-8501, Kanagawa, Japan*

<sup>c</sup> *Center for Integrated Technology Support, Nagaoka University of Technology, Kamitomioka  
1603-1, Nagaoka 940-2188, Japan*

---

**\* Author to whom correspondence should be addressed:**

Tel: +81-258-47-9345; Fax: +81-258-47-9300, E-mail: tagaya@mst.nagaokaut.ac.jp

## **Experimental Procedure S1**

Poly (amic acid) solution was diluted with NMP to 2.5 wt %, and subsequently, the diluted poly(amic acid) solution was spin-coated at 6000 rpm using a spincoater (MS-A100, Mikasa Co., Ltd.) on the glass and silicon substrates. Before the coating, the substrates were pretreated with UV/ozone (ASM401N, Azumi Giken Ltd., emitted wavelengths: 184.9 and 253.7 nm) exposure for 5 min. Then, the substrates were predried at 45 °C for 5 min, dried at 120 °C for 20 min, and baked at 200 °C for 1 h in air to obtain the PI films. Here, the chemical structure of PI is shown. Subsequently, the PI films were rubbed by a rubbing treatment machine (MRG-100, EHC Corp.) to obtain the rubbed PI (R-PI) films. For details of the rubbing treatment, the rayon-made rubbing cloth (Ageha Textile Industry Co., Ltd.) with a filament length of 1.8 mm and a density of 24,000 cm<sup>-2</sup> was used. The pile impression was defined as the depth of the deformed filaments with the pressed contact from the starting height point, and the contact distance between the filament top and the substrate surface was set at 0.1 mm. The rubbing was repeatedly treated four times, and the other rubbing conditions were set at rotation speed of 600 rpm and a stage moving speed of 15 mm s<sup>-1</sup>.

**Synthesis of the MPS Films.** MPS films were synthesized according to our previous report.<sup>18</sup> In detail, the precursor solutions were prepared by mixing TEOS, ultrapure water, ethanol, HCl, P123, and Brij 56, where the molar proportion was (TEOS) 1: (ultrapure water) 1.5: (ethanol) 4: (HCl)  $6 \times 10^{-3}$ : (P123)  $9 \times 10^{-3}$ : (Brij 56)  $2.7 \times 10^{-2}$ . Then, the prepared precursor solutions were spin-coated at 6000 rpm on the R-PI film, subsequently dried at 40 °C for 18 h, and calcinated at 350 °C for 6 h in air. According to the previous research in our group,<sup>18</sup> the FT-IR spectra of the MPS film before and after calcination (350 °C) were measured. It showed that absorption bands due to the asymmetric and symmetric stretching modes of C–H in P123 and C–H in Brij 56 were observed before calcination. In contrast, these absorption bands disappeared after calcination, suggesting that the surfactants were removed by calcination. Here, the synthesized 1-layer film was named **1L-MPS**. Moreover, the R-PI film was formed on **1L-MPS** again by the above method. Here, rubbing direction (RD) was perpendicular to the RD of the first Layer-PI. After that, the MPS precursor fluid was spin-coated, dried, and calcinated as above conditions to synthesize a 2-layer film, which was named **2L-MPS**.

---

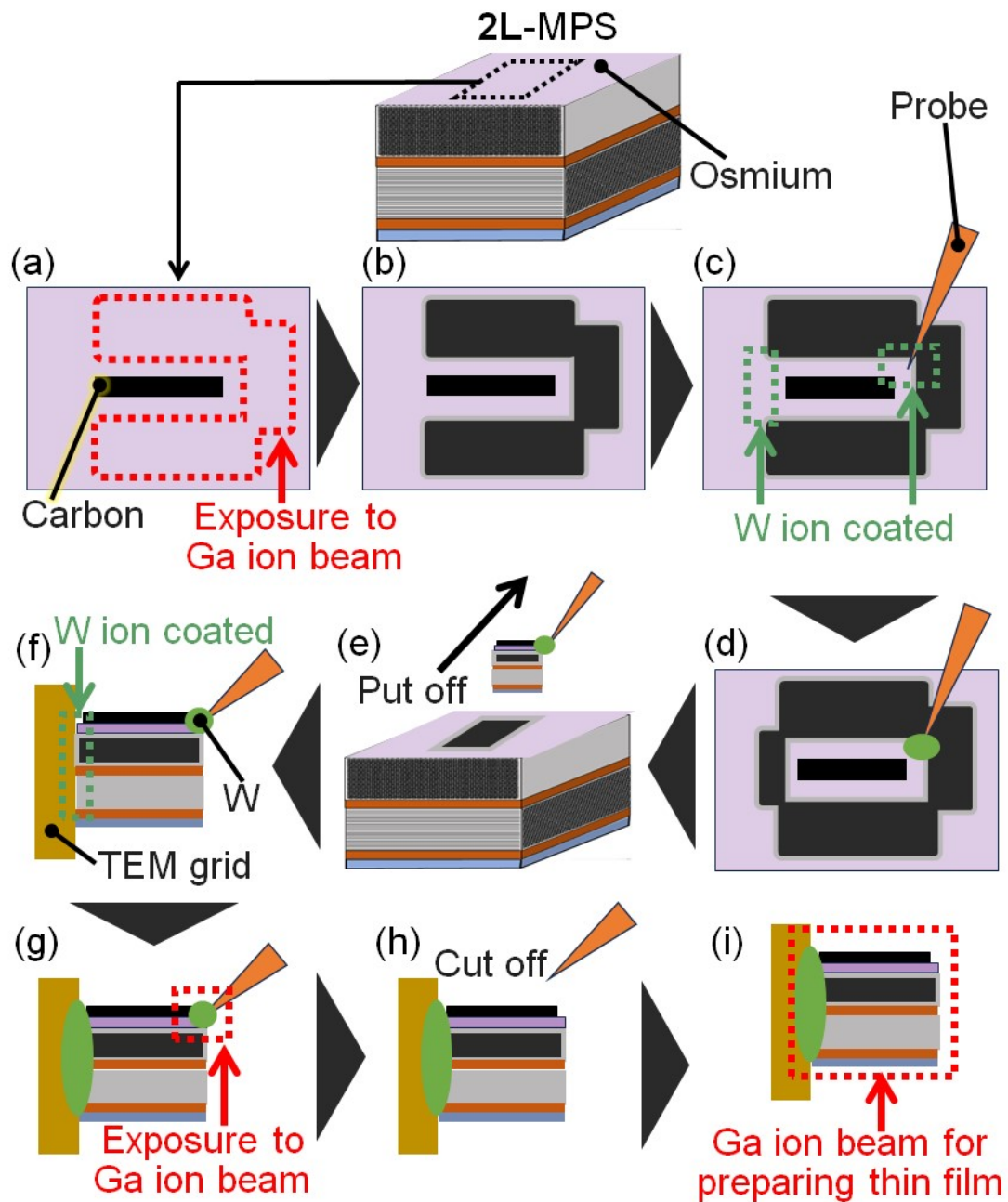
## **Reference**

- S1 R. Nakajima, Y. Chai, A. Endo, Y. Zhou and M. Tagaya, *ACS. Appl. Nano. Mater.*, 2023, **6**, 14267–14277.

## ***Experimental Procedure S2***

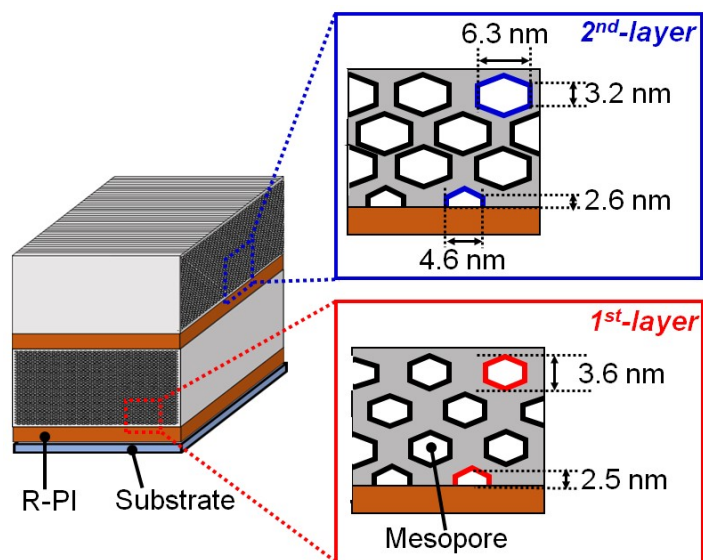
**2L**-MPS was osmium-coated with the thickness of approximately 15 nm (osmium coater: MEIWAFOSSIS Co., Ltd, Tennant20). Then, the thin films were prepared for the TEM observation by the focused ion beam / field emission scanning electron microscope (FIB/FE-SEM, JEOL Ltd., JIB-4700F). Specifically, the observation site of the osmium-coated **2L**-MPS was selected from the FE-SEM images and marked by coating the protective carbon film on the sites with the area of  $2 \times 10 \mu\text{m}^2$ . The surrounding surfaces around the protective films were then etched with the Ga ion beam and cut out as the thin film with the thickness of approximately 4  $\mu\text{m}$ . The intensity of the Ga ion beam was carefully reduced when cutting close to the thin film section in order to suppress the scratches caused by the etching process. While observing the SEM and FIB images, the tip of the nanomanipulator (Oxford INSTRUMENTS Co., Ltd., OmniProbe OP350) was then contacted with the edge section of the thin film. On this contact area, tungsten thin layer was formed by FIB-induced deposition using  $\text{W}(\text{CO})_6$  as a precursor to adhere the nanomanipulator to the thin film edge section and then was picked up from the **2L**-MPS. While observing the SEM and FIB images, the picked-up thin film was contacted with the TEM grid (material: Mo, diameter: 3 mm, thickness: 50  $\mu\text{m}$ , Nissin EM Co., Ltd.) and then exposed to the Ga ion beam to adhere the picked-up thin film to the TEM grid. Moreover, the adherent section between the nanomanipulators and the edge of the thin film is cleaved by the Ga ion beam, producing the states where only the thin film fixed to the TEM grid. The fixed thin film on the TEM grid was then etched to the thickness of 0.2  $\mu\text{m}$  by exposing to the Ga ion beam. Here, the sample stage was changed to the cooling stage (IB-Z200451APCS, JEOL Ltd.) in order to suppress the thermal damage, and the thin film was exposed to the Ga ion beam under the condition of  $-51 \text{ }^\circ\text{C}$  with adjusting the beam intensity and the acceleration voltage. The thin film was observed by transmission electron microscopy (TEM, Hitachi High-Tech Corporation, HT7700) at the acceleration voltage of 100 kV.

**Scheme S1**



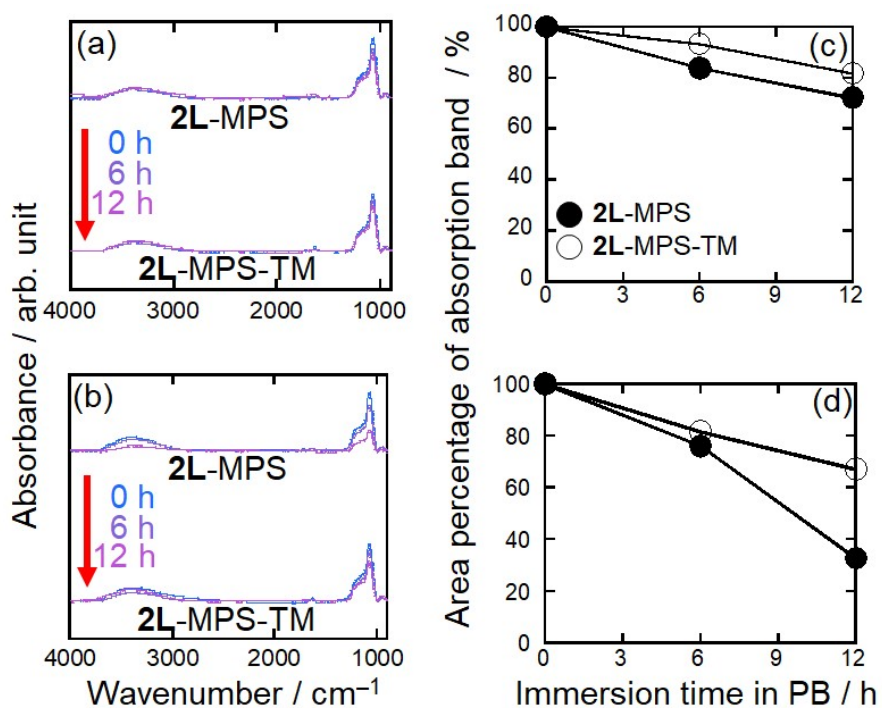
**Scheme S1.** Illustration of the thin film preparation process by the FIB and FE-SEM techniques for the TEM observation.

**Scheme S2**



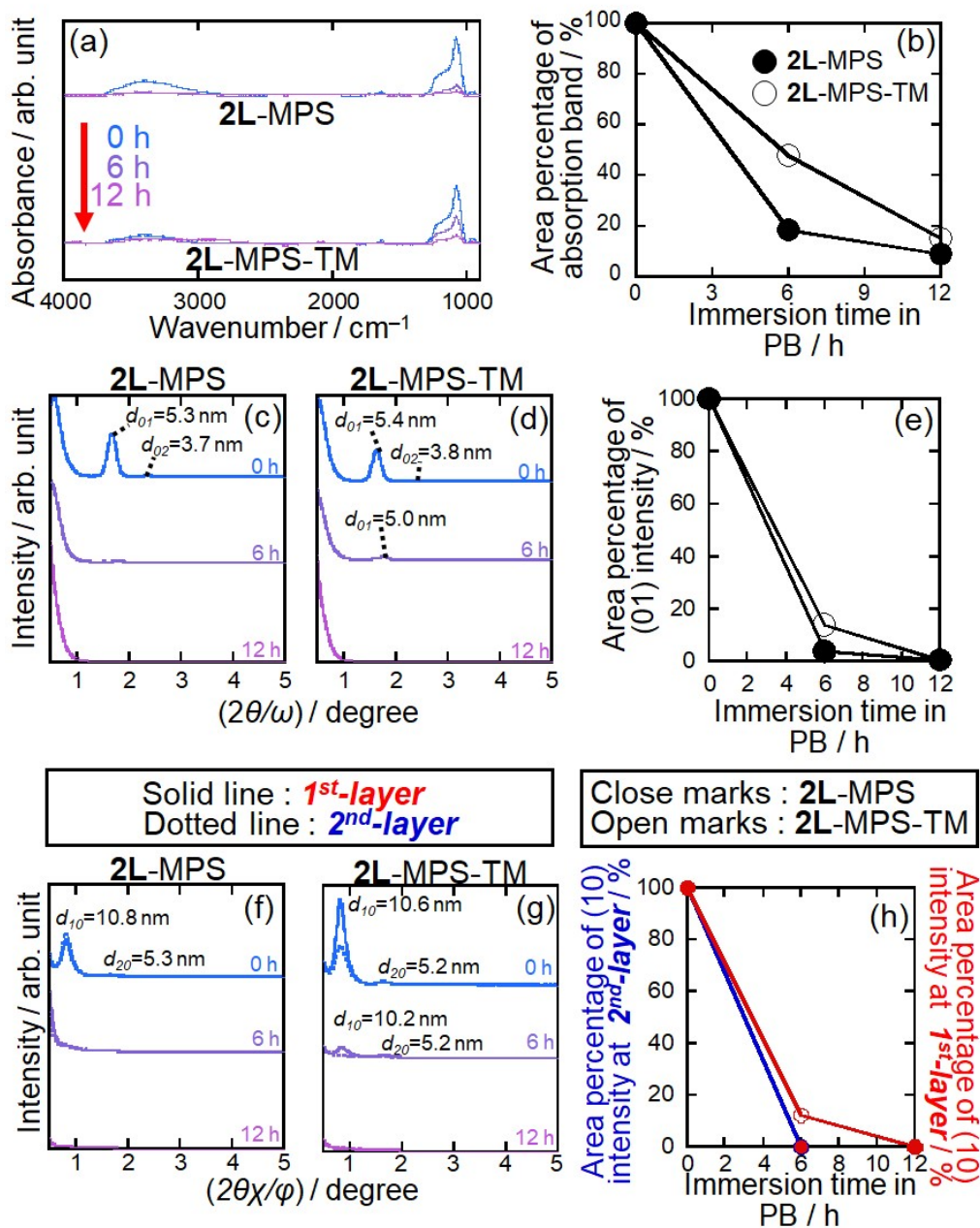
**Scheme S2.** Illustration of the mesostructures of 2L-MPS obtained from TEM images (Figure 1).

**Figure S1**



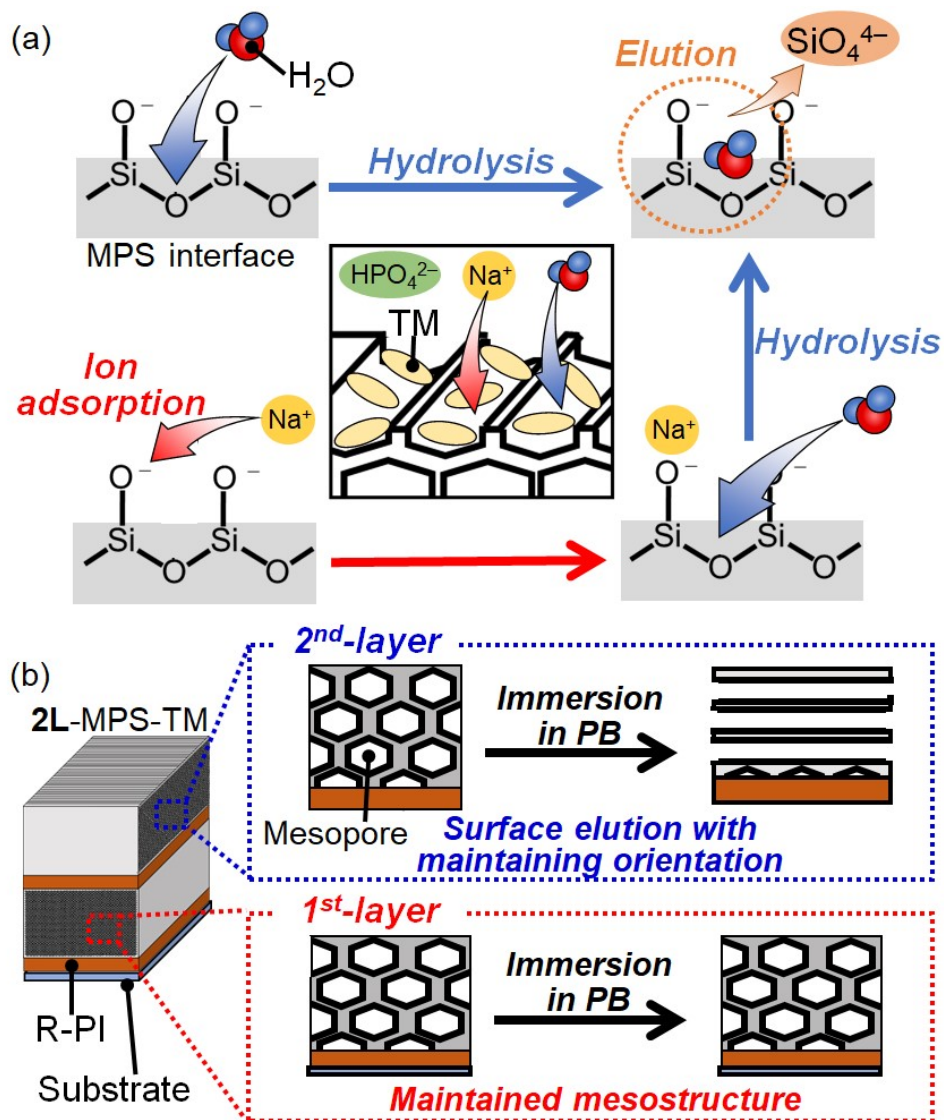
**Figure S1.** (a, b) FT-IR spectra and (c, d) Si-O-Si (996–1324 cm<sup>-1</sup>) absorption band area percentage changes of **2L-MPS** and **2L-MPS-TM** with the immersion time in the (a, c) 0.01 M-PB (pH 5.8), and (b, d) 0.1 M-PB (pH 5.8).

**Figure S2**



**Figure S2.** (a) FT-IR spectra of **2L-MPS** and **2L-MPS-TM** and (b) the Si–O–Si (996–1324  $\text{cm}^{-1}$ ) absorption band area percentage changes with the immersion time in 0.1 M-PB (pH 7.0), and (c, d) *out-of-plane* and (f, g) *in-plane* XRD patterns of (c, f) **2L-MPS** and (d, g) **2L-MPS-TM**, and the (01) diffraction peak area percentage changes from (e) *out-of-plane* and (f) *in-plane* patterns with the immersion time.

**Scheme S3**



**Scheme S3.** Illustration of (a) elution mechanism of the MPS surfaces with the immersion in PB, and (b) the mesostructural changes of 2L-MPS-TM with the immersion.